Report

Cell Reports

Nontemplated Nucleotide Additions Distinguish the Small RNA Composition in Cells from Exosomes

Graphical Abstract

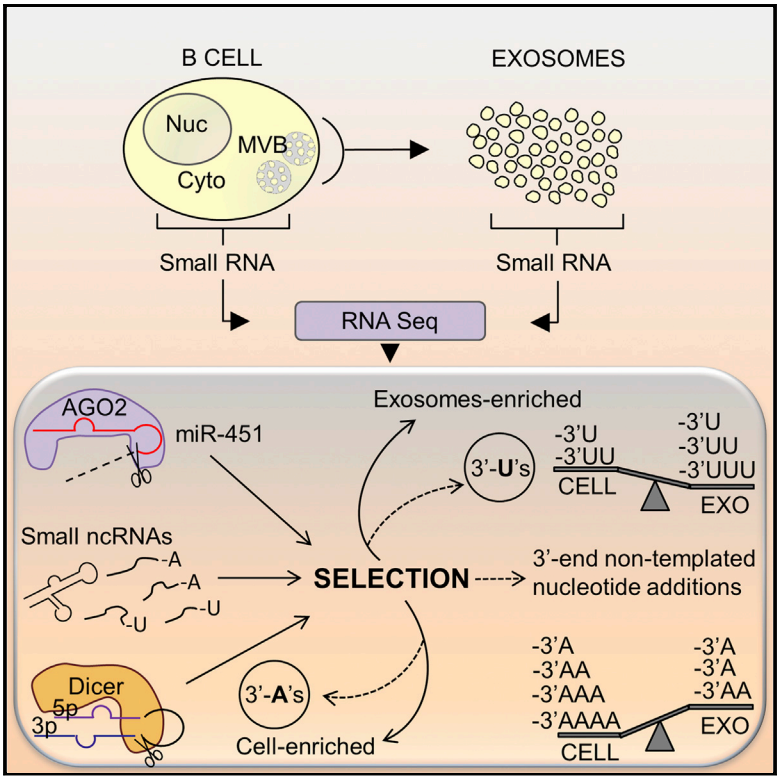

Highlights

Small ncRNAs are nonrandomly distributed in B cells and their released exosomes

3′-end adenylated miRNA isoforms are relatively enriched in cells

3′-end uridylated miRNA isoforms are overrepresented in exosomes

Nucleotide addition may affect the relative abundance of ncRNAs in cells and exosomes

Authors

Danijela Koppers-Lalic, Michael Hackenberg, ..., Gerrit A. Meijer, D. Michiel Pegtel

Correspondence

d.koppers@vumc.nl (D.K.-L.),
d.pegtel@vumc.nl (D.M.P.)

In Brief

Small RNA composition in cells differs from that in exosomes, but selection mechanisms are unknown. Koppers-Lalic et al. now demonstrate that nonrandom intra- and extracellular microRNA distribution is directed by 3′ end nucleotide additions.

Koppers-Lalic et al., 2014, Cell Reports 8, 1649–1658
September 25, 2014
http://dx.doi.org/10.1016/j.celrep.2014.08.027

Cell Reports
Report

Nontemplated Nucleotide Additions Distinguish the Small RNA Composition in Cells from Exosomes

Danijela Koppers-Lalic,[1,2,*] Michael Hackenberg,[3] Irene V. Bijnsdorp,[4] Monique A.J. van Eijndhoven,[1,2] Payman Sadek,[1,2] Daud Sie,[1] Nicoletta Zini,[5] Jaap M. Middeldorp,[1] Bauke Ylstra,[1] Renee X. de Menezes,[6] Thomas Würdinger,[7,8] Gerrit A. Meijer,[1] and D. Michiel Pegtel[1,2,*]
[1]Department of Pathology
[2]Exosomes Research Group
VU University Medical Center, 1007MB Amsterdam, the Netherlands
[3]Department of Genetics, Computational Genomics and Bioinformatics Group, University of Granada, Granada 18071, Spain
[4]Department of Urology, VU University Medical Center, 1007MB Amsterdam, the Netherlands
[5]CNR-National Research Council of Italy, IGM, and SC Laboratory of Musculoskeletal Cell Biology, IOR, 40136 Bologna, Italy
[6]Department of Epidemiology and Biostatistics, VU University Medical Center, 1007MB Amsterdam, the Netherlands
[7]Department of Neurosurgery, Neuro-Oncology Research Group, VU University Medical Center, 1007MB Amsterdam, the Netherlands
[8]Department of Neurology, Massachusetts General Hospital and Harvard Medical School, Charlestown, MA 02129, USA
*Correspondence: d.koppers@vumc.nl (D.K.-L.), d.pegtel@vumc.nl (D.M.P.)
http://dx.doi.org/10.1016/j.celrep.2014.08.027

SUMMARY

Functional biomolecules, including small noncoding RNAs (ncRNAs), are released and transmitted between mammalian cells via extracellular vesicles (EVs), including endosome-derived exosomes. The small RNA composition in cells differs from exosomes, but underlying mechanisms have not been established. We generated small RNA profiles by RNA sequencing (RNA-seq) from a panel of human B cells and their secreted exosomes. A comprehensive bioinformatics and statistical analysis revealed nonrandomly distributed subsets of microRNA (miRNA) species between B cells and exosomes. Unexpectedly, 3′ end adenylated miRNAs are relatively enriched in cells, whereas 3′ end uridylated isoforms appear overrepresented in exosomes, as validated in naturally occurring EVs isolated from human urine samples. Collectively, our findings suggest that post-transcriptional modifications, notably 3′ end adenylation and uridylation, exert opposing effects that may contribute, at least in part, to direct ncRNA sorting into EVs.

INTRODUCTION

The human genome encodes for a vast amount of small non-protein-coding RNA (ncRNAs) transcripts. Multiple ncRNA classes exist that include the highly abundant tRNAs, rRNAs, small nucleolar RNAs, microRNAs (miRNAs), small interfering RNAs, small nuclear RNAs, and piwi-interacting RNAs (piRNAs) (Amaral et al., 2008; Martens-Uzunova et al., 2013). The 22 nt long miRNAs gained much attention acting as potent translational repressors by binding to target mRNAs by sequence complementary (Ameres et al., 2007). The activity of miRNAs is related to their concentration in the cytoplasm and interaction with RNA-induced silencing complexes (RISC) (Mullokandov et al., 2012). Subtle alterations in the levels of miRNAs may already influence cellular processes, whereas strong perturbations can cause disease. Besides abundance RNA-binding proteins, RNA partners and subcellular localization are additional factors controlling miRNA physiology (Wee et al., 2012).

We previously reported that Epstein-Barr virus (EBV)-transformed lymphoblastoid B cells (LCLs) constitutively secrete large quantities of endosome-derived exosomes that incorporate both human and viral miRNAs. Copy-number measurements demonstrated that these exosomes mediate cell-cell transmission of miRNAs, leading to viral miRNA accumulation in recipient cells and target mRNA repression (Pegtel et al., 2010). Together with following observations using different systems, they strongly suggest that miRNA transfer via exosomes can have a role in cell-cell communication (Mittelbrunn and Sánchez-Madrid, 2012). Small RNAs are presumably sorted into exosomes at endosomal membranes because interfering with their formation affects functional transfer (Kosaka et al., 2013; Mittelbrunn et al., 2011; Okoye et al., 2014). Although secretion of miRNAs with extracellular vesicles (EVs) may occur in a nonrandom fashion (Bellingham et al., 2012; Nolte-'t Hoen et al., 2012), a thorough comparative analysis in purified exosome populations and the producing cells has been lacking. Demonstrating potential mechanisms for selective sorting of small RNAs into exosomes would be relevant to understand their gene-regulatory function in both the producing and recipient cells (Pegtel et al., 2011) and may provide clues on their mobility in living organisms (Chitwood and Timmermans, 2010).

In a prior study, we observed that certain miRNA species are precluded from exosome incorporation, suggesting selection of miRNA for exosomal release. Because RISC complexes are physically and functionally coupled to endosomal membranes in flies and humans (Gibbings et al., 2009; Lee et al., 2009) and because GW182 knockdown reduces miRNA secretion through exosomes (Yao et al., 2012), it appears that intracellular

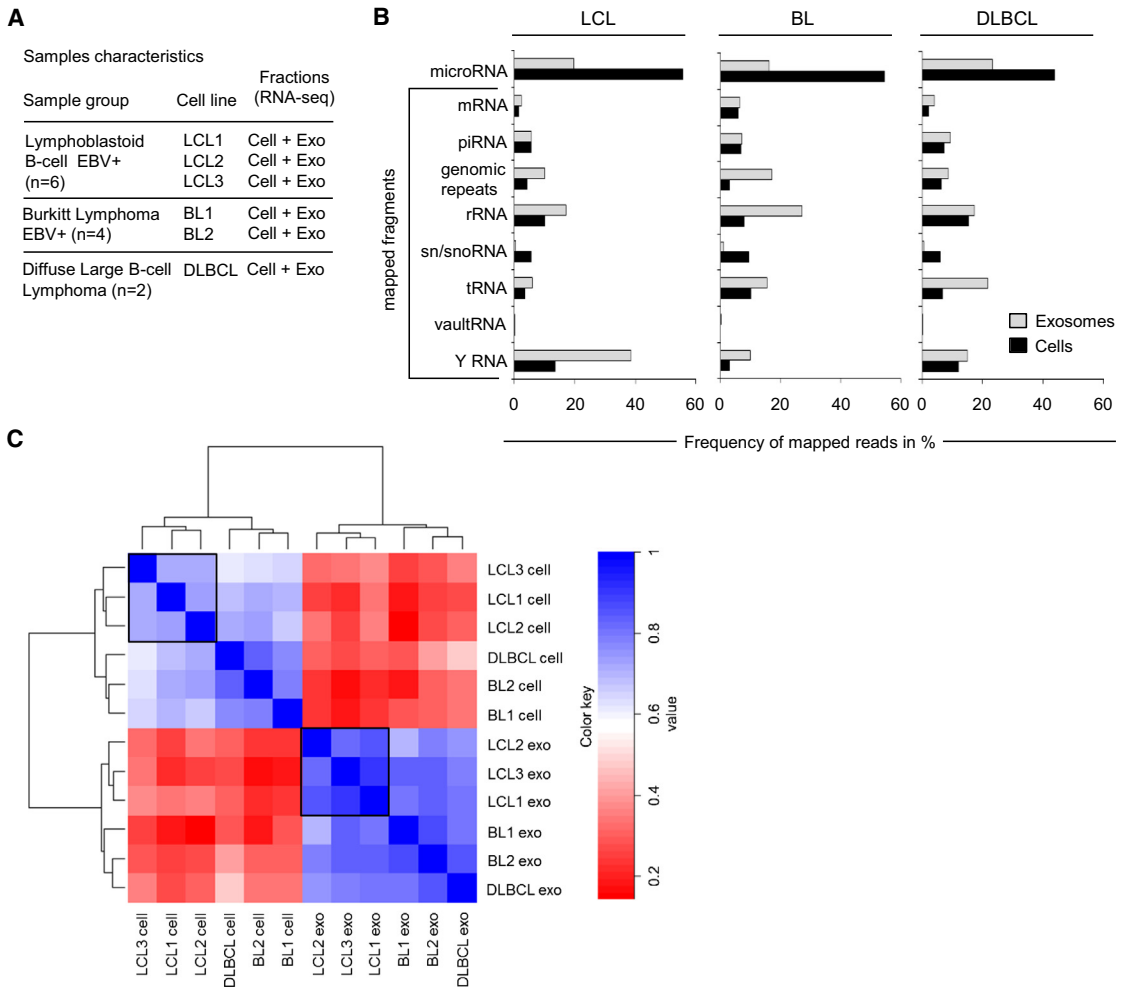

Figure 1. Small RNA Repertoire from B Cells and Their Exosomes

(A) cDNA libraries were generated from cellular and exosomal small RNA fractions. Sample groups, cell lines, and a type of sample fraction are indicated (see also Table S1A).

(B) All mapped reads from cellular and exosomal fractions are grouped by annotation to RNA transcripts of origin and presented as distribution frequency of mapped reads in percentage.

C) Heatmap showing the pairwise Spearman (rank) correlation between miRNAs expression per 12 libraries. Upper left square: LCL cells (n = 3; r = 0.76–0.8); lower right square: LCL exosomes (n = 3; r = 0.72–0.76).

trafficking, localization, and activity control small ncRNA release. Recent studies suggest that nontemplate terminal nucleotide additions (NTAs) predispose miRNA association with RISC (Burroughs et al., 2010; Polikepahad and Corry, 2013), affecting their stability, turnover, and activity (Ameres et al., 2010; Baccarini et al., 2011; Boele et al., 2014; Jones et al., 2009). Because adenylation effects the stability and activity of certain miRNAs (Boele et al., 2014; D'Ambrogio et al., 2012), we hypothesized that nonrandom incorporation of miRNAs into mammalian exosomes could be coupled to their activity and posttranscriptional modification by NTAs.

Here, we report that 3′ end adenylation of defined miRNA species is correlated with relative enrichment in cells compared to exosomes. This is consistent with this type of modification hindering incorporation and secretion of these miRNA isoforms via exosomes. Importantly, we found an opposite behavior for 3′ end uridylated miRNA isoforms, which appear enriched in exosomes. Our study provides a new understanding of exosomal small RNA cargo and offers a rationale for studying miRNA processing, modification, and turnover in connection to exosome biology.

RESULTS

Small Noncoding RNA Families Are Differentially Distributed between B Cells and Exosomes

To determine whether small RNA species of less than 200 nt are enriched in exosomes, we generated cellular and corresponding exosomal small RNA libraries for sequencing of EBV-driven LCLs and B cell lymphoma cell lines (Figure 1A). This approach provided a comprehensive data set to perform high-powered statistical analysis on the intra- and extracellular RNA repertoires

within a defined cellular background (individual reads and alignment statistics in Table S1). Comparison to RNA reference libraries revealed that cellular and exosomal small RNA fractions contained products from diverse classes of RNAs (Figure 1B). Besides their large diversity, it seems that several RNA classes are enriched in cells (Figure 1B; black bars), whereas others are overrepresented in exosomes (gray bars). In all cellular samples, the class of miRNAs represents around 50% of the small RNA pool. In exosomes, however, miRNAs appear to be underrepresented (20%) in comparison to other small RNA fragments. RNA elements derived from the other ncRNA classes (i.e., tRNAs, piRNAs, rRNAs, Y RNAs, and vault RNAs) were generally enriched in the exosomes, even though the class distribution was distinct between cell types (Figure 1B).

The most striking distinction between LCL and lymphoma exosomes was the extreme abundance of human Y RNAs fragments (38%; Figures 1B and S1A; $p < 0.05$). To investigate whether the enrichment of Y RNA fragments (Figure S2B) reflects the presence of full-length transcripts, we performed semiquantitative RT-PCR on the exosomal RNA that was subjected to sequencing. We detected high levels of full-length Y RNA species (i.e., RNY1, RNY3, RNY4, and RNY5) and vault RNA1-1 (Figure S2C) in exosomes. These data are consistent with previous observations in exosomal small RNA sequencing studies (Bellingham et al., 2012; Nolte-'t Hoen et al., 2012; Vojtech et al., 2014). Although the biological relevance of Y RNAs incorporation in exosomes is currently unclear, these small regulatory RNAs seem to be specifically packaged in enveloped and nonenveloped viral particles (Garcia et al., 2009). The selective recruitment of small ncRNAs from the host cell into (retro) viral particles and exosomes implies that common molecular mechanisms may drive their packaging process. This realization could aid future characterization of cellular components governing exosomes biogenesis and cargo selection (Koppers-Lalic et al., 2013).

High and Low Abundant MicroRNAs Are Nonrandomly Incorporated into Exosomes

To gain more insight into possible disparities between miRNA distribution in cells versus exosomes, we calculated Spearman correlations between normalized miRNA reads of all cellular samples and paired exosomes ($n = 12$). Cluster analysis separated the LCL samples from the lymphoma samples, as illustrated by the heatmap correlation matrices (Figure 1C; Spearman correlations [r] = 0.48–0.81 range), showing high level of correlation between LCL data sets ($r = 0.72–0.8$).

Next, mapped miRNA counts were fitted in a generalized linear model using the R package edgeR (Robinson et al., 2010) and the relative abundance of individual miRNAs in cells and exosomes were compared (Tables S1B and S1C). The most abundant cellular miRNAs (relative expression >10,000 reads per million [RPM] normalized to the total miRNAs reads) in general represented the most abundant miRNAs in the exosomes (Table S1B). Although the miRNA distribution in exosomal fractions is clearly influenced by cellular miRNA abundance, we identified a subset of miRNAs that were discordantly distributed between cells and exosomes (false discovery rate [FDR] < 0.05; Tables S1B and S1C).

To investigate which miRNAs are relatively enriched in LCL, Burkitt lymphoma (BL), and diffuse large B cell lymphoma (DLBCL) backgrounds, all miRNAs were grouped according to the fold enrichment in exosomes versus cellular miRNA reads (RPM). We determined that the most significant enrichment of miRNAs was observed in exosomes rather than in cells (Figure 2A). To assess whether discordantly distributed miRNAs (Figures 2B and 2C) are detectable by other methodologies, we performed stem-loop-based quantitative RT-PCR (qRT-PCR) on RNA extracted from LCL cells and exosomes (LCL1 biological duplicates). The PCR data analysis showed that human miRNAs miR-451, miR-127-3p, and miR-410 were relatively abundant in exosomes fractions, which is consistent with the RNA sequencing (RNA-seq) approach. Strikingly, miR-451 and miR-127-3p were barely detectable in cells, in contrast to preferentially cell-enriched miRNAs miR-1275 and miR-744 (Figure 2D). The enrichment of miR-127-3p in exosomes could be related to its function as a negative regulator of B cell lymphoma 6 mRNA (BCL6), a transcriptional repressor in lymphomagenesis and miR-127-3p release, could favor the growth and survival of B cell lymphoma cells (Saito et al., 2006).

Differences in Human and Viral miRNA Distribution

EBV-miRNAs provide essential growth advantages to EBV-infected proliferating B cells and EBV-driven lymphomas (Qiu et al., 2011; Seto et al., 2010), and we expected these to be relatively enriched in cells. To analyze the distribution of 44 miRNAs encoded by EBV in the transformed B cells, we calculated the fold change (FC) by means of edgeR, i.e., using trimmed mean of M values normalization for miRNA reads only. This is illustrated in Figure 2E, where the majority of viral miRNAs (indicated in red) have a tendency toward cell enrichment (negative log2 FC). In contrast to human miRNAs, not a single viral miRNA was found significantly enriched in exosomes (Figure S2B). EBV-miRNA abundance varies widely, yet most abundant ones belonged to the BART cluster miRNAs (Table S1D) that target 132 apoptosis-related cellular mRNAs, in agreement with these EBV miRNAs promoting B cell survival (Riley et al., 2012).

3′ End NTAs Define Retention or Release of miRNAs In Vitro and In Vivo

Whereas the most abundant miRNA sequence from pre-miRNA hairpins is usually referred to as the "mature" miRNA (miRBase), inefficient Drosha or Dicer-mediated processing of pre-miRNAs produces 3′ end length variants (e.g., truncations and elongations). Additional miRNA isoforms are generated by nucleotidyl transferase-mediated posttranscriptional modifications known as nontemplated terminal NTAs (Burroughs et al., 2010; Morin et al., 2008; Wyman et al., 2011; Figure S3A).

Global analysis of miRNA 3′ end variations showed that 3′ end length isoforms are equally distributed between cells and exosomes, in contrast to miRNAs with 3′ end NTAs that exhibited differential distribution. The comparison of individual NTA types (i.e., A, U, C, or G) to the sum of all reads with NTAs showed an enrichment of adenylated miRNA isoforms in the cellular fractions. In contrast, 3′ end uridylated miRNAs were overrepresented in exosomes of all LCL samples analyzed (Figure 3A). To analyze whether the proportion of NTA-modified reads

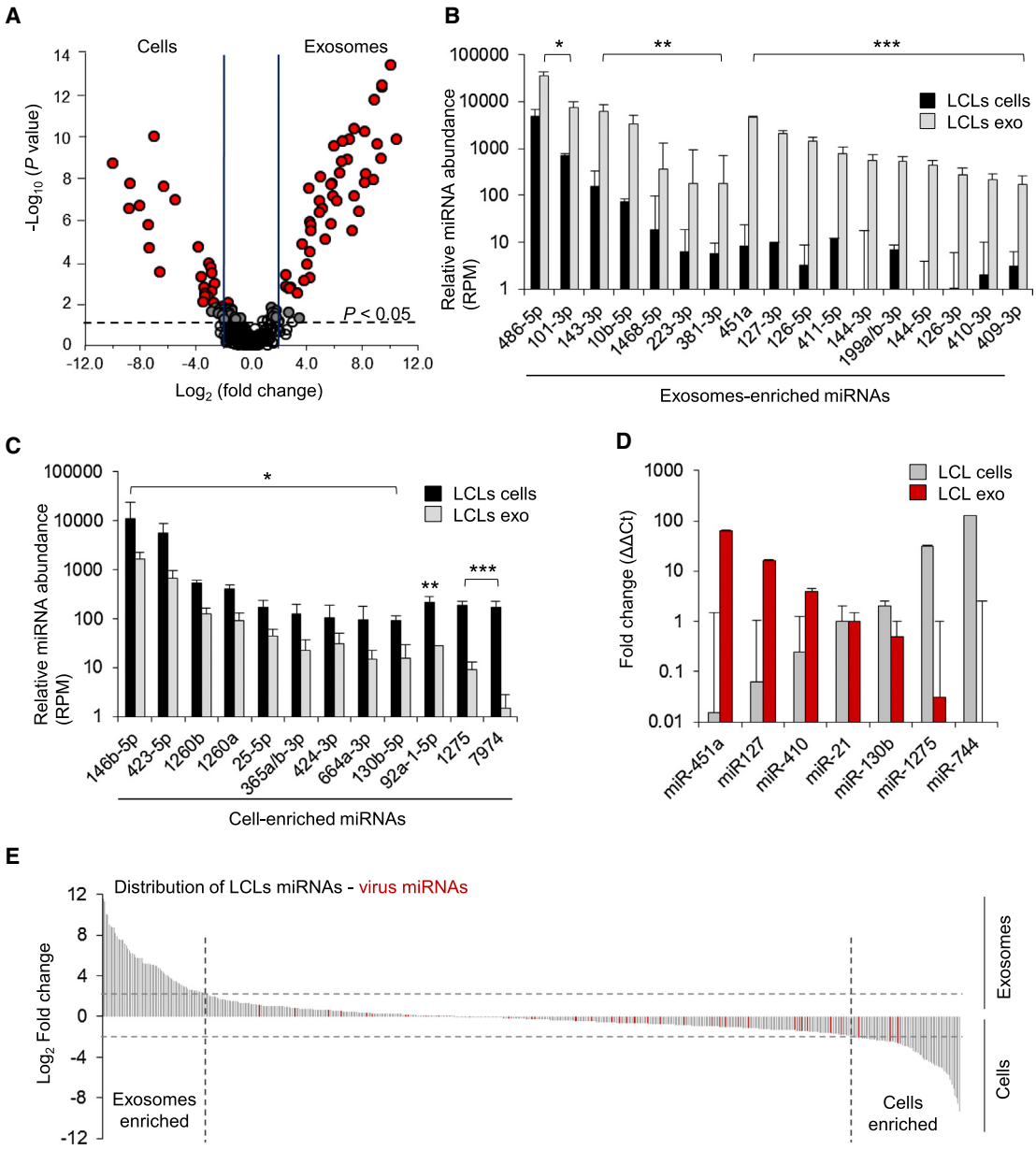

Figure 2. MicroRNAs Are Nonrandomly Incorporated into Exosomes

(A) Volcano plot of significantly differentially abundant miRNAs in B cells and their secreted exosomes. Individual miRNAs from all samples were classified according to the fold change (log2 of exo/cell ratio) at the x axis and plotted against their individual p value (y axis). Red dots: miRNAs in cells or exosomes ($p < 0.001$); gray dots: miRNAs in cells or exosomes at $p < 0.05$. Vertical lines: >4-fold enrichment in cells (left) or exosomes (right).

(B and C) Significant overrepresented miRNAs in exosomes and cells from LCLs samples are depicted at the x axis with their read abundance exceeding 100 RPM (y axis on logarithmic scale). The error bars are the SD of the mean (n = 3); *$p < 0.05$; **$p < 0.005$; ***$p < 0.0005$; ns, not significant (Student's t test); FDR < 0.05 (see also Table S1C).

(D) miRNA detection in LCL cells and their matching exosomes by stem-loop-based qRT-PCR. Data represent ΔΔCt value of technical duplicates normalized to miR-92a Ct value from two independent experiments (n = 4; error bars ± SEM; $p < 0.05$).

(E) Human (LCLs) and EBV miRNAs were classified according to the fold change (log2 FC) between cellular and exosomal miRNAs; vertical dotted lines: miRNA fractions with >4-fold enrichment in cells or in exosomes; red bars: virus miRNAs.

(A, U, C, or G) differs significantly between cell and exosome samples, each miRNA sequence with 3′ end NTAs was extracted from all 12 samples (LCLs: n = 6; BLs: n = 4; DLBCL: n = 2) and fitted in a logistic model, which also corrected for the cell line effect (accounting for the paired design). The results suggest that 3′ end adenylated miRNA isoforms are preferentially retained (chi-square test; $p < 0.05$), whereas all other NTAs are preferentially released (3′ end-U: chi-square test, $p = 0.02$;

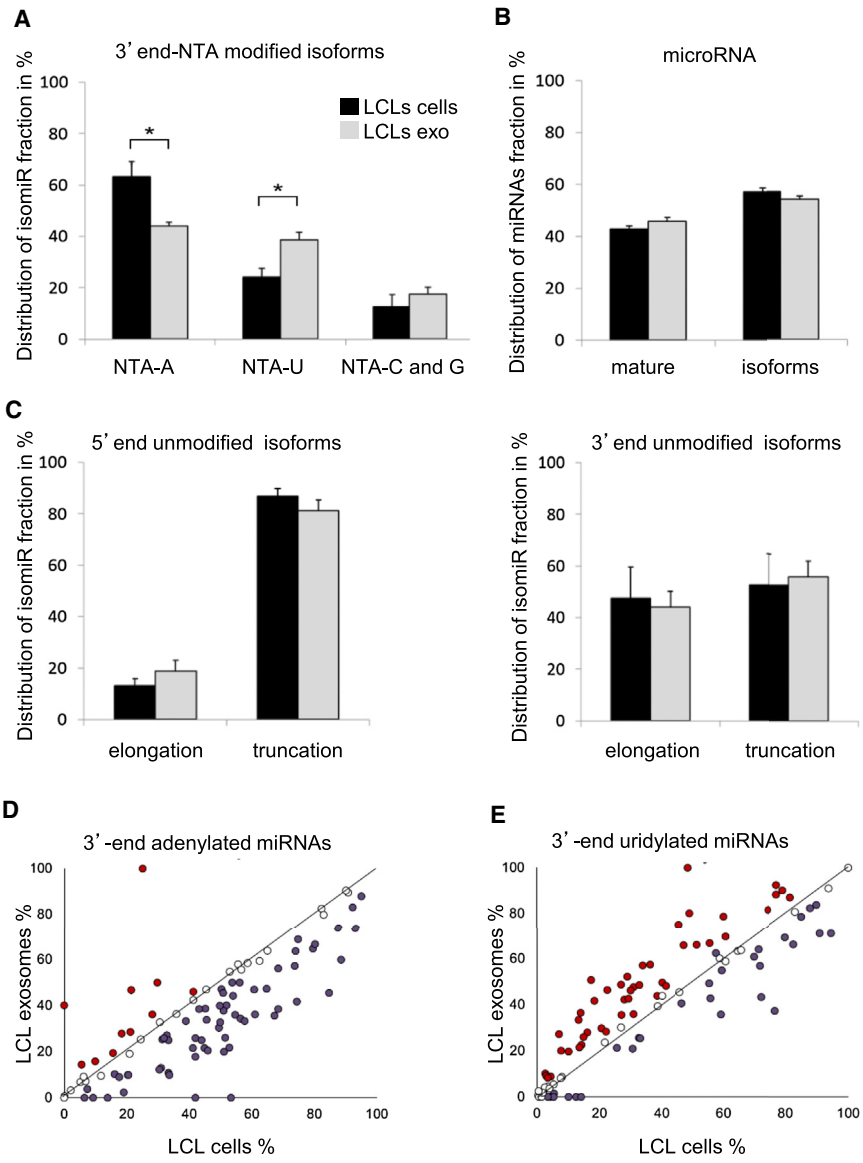

Figure 3. The 3′ End Posttranscriptional Modification Distinguishes Cellular and Exosomal miRNA Repertoire

(A–C) Distribution of mature miRNAs and their NTA-modified or unmodified isoforms in LCL samples (biological triplicates) was compared between cells and exosomes. The error bars are the SD of the mean (LCL 1–3 samples; n = 3); *p = 0.005 (Student's t test).

(D and E) Frequency plots of a pairwise analysis of 3′-A and 3′-U isoforms. miRNAs found to be expressed in both cells and exosomes were selected (at ≥300 reads, 100 miRNAs) for distribution analysis of their adenylated and uridylated reads expressed as percentage to the total of all NTA-modified reads. Red circles: isoforms with higher percentage in exosomes; purple circles: isoforms with higher percentage in cells; white circles: equal distribution.

3′ end-C: Fisher's exact test, p = 0.04; 3′ end-G: Fisher's exact test, p = 0.02; Figure S3B). It must be noted that nonadenylated isoforms in exosomes may also be overrepresented in exosomes versus cells if their stability is lower in cells.

Apart from a global NTA distribution analysis, in three LCL samples (i.e., biological triplicates), we observed that the disparity of 3′ end adenylated or uridylated miRNA isoforms between cells and exosomes was significant (p = 0.005; Student's t test; Figure 3A) and not observed for mature miRNA (miRBase-based annotation) sequences (Figure 3B) or unmodified (elongated or truncated) isoforms (Figure 3C). To examine the effect of 3′ end NTAs on distribution of individual miRNAs, we analyzed 100 abundantly expressed miRNAs in both cells and exosomes and then matched cellular miRNAs to miRNAs in exosome fractions for a pairwise analysis. The results demonstrated that sequences of individual miRNAs with 3′ end adenylation are more associated with cellular fractions (Figure 3D), whereas the same miRNAs but with 3′ end uridylation are more prone to enrichment in exosomes (Figure 3E). We thus conclude that the type of added nucleotide, i.e., adenine or uridine, distinguishes the distribution in cells from exosomes.

Deeper analysis of individual miRNA sequences allowing more mismatches and longer flanking regions (+6 nt) outside the miRBase-annotated 3′ end sequence revealed that 3′ ends of many miRNAs are extended with more than one nontemplate nucleotide. To address whether the number of posttranscriptionally added nucleotides has a cumulative effect on the distribution, we first calculated the ratio of the fold changes between cells and exosomes (defined as enrichment coefficient; see Experimental Procedures) for sequence reads with a particular NTA type with nonmodified forms, taking into account the number of added nucleotides. 3′ end adenylation increases the probability for retention, and this probability increases proportionally with the number of added A's (Figure 4A). Strikingly, triadenylated human miRNAs were significantly more frequent in LCL cells than in the corresponding exosomes (Figure 4A; p < 0.001; Student's t test), whereas triadenylated viral miRNAs are mainly detected in LCL cell fractions (Figure S4). The association of 3′ end adenylation with an increase in cellular enrichment of viral miRNAs further supports our prior suggestion that viral miRNAs exhibit a strong tendency to remain cell associated (Figures 2E, S2B, and S2C).

In contrast to 3′ end adenylation, the disproportional occurrence of small RNAs with uridines at the 3′ ends seems to define exosomal RNA cargo (Figures 4A and 4B). To investigate whether this is not a phenomenon restricted to B cells in culture,

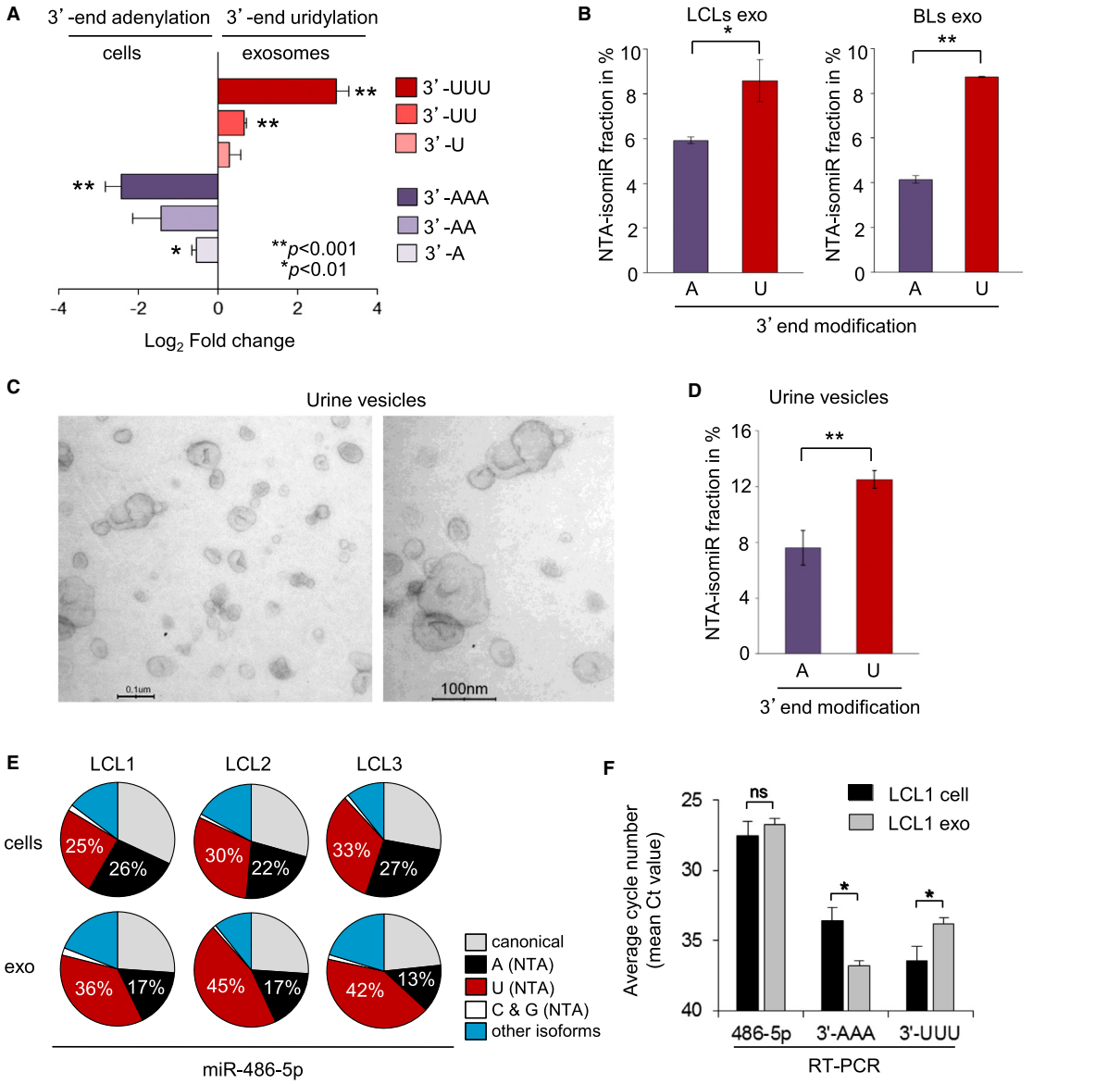

Figure 4. The Extent of 3′ End Adenylation Coincides with Cellular Enrichment whereas 3′ End Uridylation Demarcates Exosomal Small RNA Cargo

(A) Fraction of human miRNAs for which the adenylated reads (3′ end-As) and the uridylated reads (3′ end-Us) show enrichment in cells or in exosomes, respectively. Enrichment coefficient defined as log2 fold change measures the enrichment of NTA reads found in exosomes or in cells when compared to the canonical read. The error bars SD for LCLs (n = 3).

(B–D) 3′ end uridylation rather than adenylation is more frequent on miRNA isoforms present in LCLs exosomes (B, left), BLs exosomes (B, right), and in human urine exosomes (D). The bars represent the weighted mean of isoforms reads per sample (exosomes only) with 3′ end NTA; nucleotide type indicated on the x axis; error bars SD for LCLs (n = 3): *p = 0.005; BLs (n = 2): **p = 0.001; human urine (n = 6): **p < 0.0001 (Student's t test). (C) Morphological characterization of EVs isolated from human urine by transmission electron microscopy; scale bar 100 nm; magnification ×30,000 (left panel) and ×50,000 (right panel).

(E) Distribution of miR-486-5p between individual LCL cells and exosomes libraries. All sequencing reads that mapped to miR-486-5p were summed, and the contribution of (iso)form types of miR-486-5p is expressed as percentage.

(F) Detection of canonical miR-486-5p, 3′ end adenylated miR-486-5p (3′-AAA), and 3′ end uridylated miR-486-5p (3′-UUU) in cellular (LCL1) and exosomal RNA fractions by qPCR. Data represent mean cycle threshold (Ct) value of technical duplicates from two independent experiments (n = 2; error bars SD; *p < 0.01; ns, not significant).

we collected and purified naturally occurring EVs from human urine (Figure 4C) using the same exosome-isolation protocol. We sequenced the small RNA content from six urine exosomes samples derived from healthy individuals (Table S2). In full accordance with 3′ end uridylation-mediated miRNA isoforms distribution observed in B cell exosomes (Figure 4B; p ≤ 0.005;

Student's t test), human urine exosomes are significantly enriched in 3′ end uridylated miRNAs (Figure 4D; $p < 0.0001$; Student's t test). We conclude that 3′ end uridylated miRNAs are overrepresented in exosomes and that relative enrichment of 3′ end adenylated miRNA isoforms in cells increases with the number of adenine nucleotides added to the 3′ end of the miRNA.

The Impact of 3′ End NTAs on Exosomal Sorting of Individual miRNAs

Whereas NTAs distinguish the miRNA distribution between cells and exosomes, the impact of NTAs on individual miRNAs may be distinct. For example, 3′ end uridylated reads of abundant exosome-enriched miRNAs 486-5p, 143-3p, and 101-3p show an above-average percentage (38%) of all uridylated isoforms present in exosomal fraction. Yet, miR-486-5p is seemingly equally distributed at the mature miRNA level (Figure 4E; in gray). Notably, 50% of all reads mapping to the mature miR-486-5p sequence are either adenylated or uridylated isoforms (Figure 4E). When using the weighted means of all miRNAs in LCL samples, we observed that triuridylated reads are nine times more frequent in LCL exosomes compared to the cellular content ($p = 0.01$; unpaired t test). We developed stem-loop-RT-PCR primers that can distinguish miR-486-5p 3′ end triadenylated and 3′ end triuridylated isoforms. As expected, mature miR-486-5p without 3′ end nucleotide additions are equally distributed, whereas 3′ end triadenylated isoforms were enriched in cells (10-fold) and 3′ end triuridylation (5-fold) in exosomes (Figure 4F). This independent approach supports the RNA-seq data (Figure 4E) and demonstrates that different types of 3′ end posttranscriptional modifications are detectable by RT-PCR. Thus, abundant miRNAs and their isoforms represent key subpopulations with unique distribution properties, depending on the type and the extent of 3′ end posttranscriptional modification.

Apart from human and viral miRNAs, we found that adenylation and uridylation can also occur at the 3′ ends of processed fragments originating from small cytoplasmic Y RNAs (Figure S3C). Importantly, most of the 3′-end-modified small RNA molecules followed the same fate as miRNA isoforms in regard to exosomal enrichment, suggesting that NTA modifications act as a small RNA sorting signal beyond the class of miRNAs. These results underscore the relevance of 3′ end NTA and expand our knowledge on diversity of small RNA substrates for the nucleotidyl-transferase family of enzymes (Martin and Keller, 2007).

DISCUSSION

In this study, we addressed the composition of small ncRNAs in human B cells and exosomes in detail. We discovered that 3′ end posttranscriptional modifications define a critical distinction between miRNA distribution in cells and exosomes both globally and at the individual miRNA level.

Unevenly distributed miRNA species between cells and their released exosomes may be functionally relevant. Although not studied here extensively, gene ontology analysis suggested that cellular miRNAs repressing the mitogen-activated protein kinase/phosphatidylinositol 3-kinase survival pathway are overrepresented in B cell exosomes (Figure S2A). Nonrandom disposal of growth-restricting miRNAs is consistent with exosomal sorting and release mechanisms for miRNAs in mammalian cells. Indeed, sequence-dependent miRNA association with exosome-incorporated RNA-binding proteins (RBPs) may promote their release (Villarroya-Beltri et al., 2013). Interestingly, AGO2 is generally absent from exosomes (Vesiclepedia: http://microvesicles.org/) and degraded by selective autophagy when dissociated from miRNAs (Gibbings et al., 2012), suggesting that miRNAs are secreted via exosomes by dissociating from or associating with particular RBPs. This is distinct from observations in human plasma where cell-free AGO2/miRNA complexes are detectable (Arroyo et al., 2011). Future studies should answer whether nonrandom miRNA release has a biological impact on gene regulation, which likely depends on multiple additional factors. Indeed, the level and function of mature miRNAs are the result of different rates of both miRNA and target transcription, processing location, and turnover (Ameres et al., 2010; Baccarini et al., 2011).

In B cells, miR-486 is a highly abundant miRNA with an extensive repertoire of adenylated and uridylated isoforms, but overall, miR-486 seemed preferentially secreted by proliferating B cells. Could this observation be reconciled in the multifaceted context of miRNA activity and biological function? The apparent accumulation of adenylated miR-486 isoforms may have physiological relevance, as EBV-driven proliferating B cells require ongoing nuclear factor (NF)-kB activation for their survival (Guasparri et al., 2008). Moreover, posttranscriptional modifications of miR-486, for example by 3′ uridylation, may indicate an antagonistic activity on NF-kB suppressors (Song et al., 2013). Whereas the functional significance of these subtle 3′ end modifications are becoming unraveled (Boele et al., 2014; D'Ambrogio et al., 2012; Jones et al., 2009; Katoh et al., 2009), their exact role in selective miRNA turnover, abundance, and activity is currently far from understood and complex (Ameres and Zamore, 2013). Differential expression of miRNAs with terminal NTAs seems to be associated with disease and can vary among different stages of embryonic development (Fernandez-Valverde et al., 2010; Wyman et al., 2011).

The observation that 3′ end adenylated miRNA species are relatively enriched in cells can be explained by 3′ end adenylation increasing small RNA stability and activity (D'Ambrogio et al., 2012; Katoh et al., 2009). Whereas adenylation seems to induce stability (Katoh et al., 2009), in plants, *Drosophila* and *C. elegans* 3′ end addition of uracil residues renders the RNAs less stable (Scott and Norbury, 2013). In mammalian cells, ZCCHC11, a terminal uridyltransferase also known as TUT4, mediates terminal uracil additions of miR-26a, thereby abolishing its function, albeit its relative abundance appears unaffected (Jones et al., 2009). Enrichment of 3′ uridylated miRNAs in exosomes may thus be explained by preferential release or could be due to a high turnover in cells compared to exosomes. In addition, uridityl transferase activity in exosomes themselves may be a cause of 3′ uridylation, although quantitative proteomic analysis argues against the presence of such enzymes in exosomes (Exocarta: http://www.exocarta.org/). It thus remains to be seen whether uridyl transferases are present

in EVs originating from different cell types. Interestingly, mature miR-451 (i.e., without NTAs) is highly abundant in exosomes, which argues against the conclusion that uridylation favors miRNA release. Provocatively, however, the mature miR-451 3′ end contains a UUU sequence, suggesting that the presence of a uracil residue itself is sufficient as sorting signal. Although additional explanations cannot be ruled out, we speculate that 3′ adenylation of defined miRNA species favors cellular retention, whereas 3′ uridylation may promote the release of miRNAs and processed Y RNAs.

Our work provides a strong rationale for studying 3′ end post-transcriptional modifications in combination with exosome biology. We and others recently provided evidence that selective secretion of signaling proteins via exosomes has an antagonizing effect on intracellular signaling pathways (Chairoungdua et al., 2010; Verweij et al., 2013). The notion that miRNA activity is dependent on the presence of selective mRNA targets and coupled to incorporation into exosomes yields new perspectives on gene regulation control. For example, deregulation of exosome production, as observed in most tumor cells (Balaj et al., 2011), may also affect miRNA function. In addition, the identification of specific modified RNAs in EVs isolated from human body fluids such as urine may also be valuable for diagnostic purposes. Deeper understanding of the underlying mechanism(s) controlling small ncRNA selection and release via exosomes may advance future biofluid-based diagnostic applications.

EXPERIMENTAL PROCEDURES

Preparation of RNA Samples for Deep Sequencing

For each cellular or exosomal sample, an equal amount of input RNA (600 ng of RNA) was prepared for sequencing using the TruSeq small RNA sample prep following manufacturer's instruction (Illumina). Sequence libraries were measured on an Agilent 2100 Bioanalyzer (Agilent Technologies), and up to 12 samples were equimolarly combined per run. Sequencing was performed on a HiSeq 2000 (Illumina) paired-end 100-cycle (PE100) run.

Detection of RNA Reads with Nontemplated Nucleotides Additions and Statistical Analysis

miRNA isoforms or isomiRs are retrieved by stepwise analysis depicted in Figure S3A. Briefly, for detection of NTAs at 3′ termini of mapped RNA elements, we compared the read sequence to the aligned pre-miRNA sequence, starting at the nucleotide position 18 of the read. If the algorithm finds a mismatch position between the read and the pre-microRNA after position 18, the read is further analyzed from the mismatch position to the end of the read whereas all following nucleotides need be equal to the one at the mismatch position. If a different nucleotide is encountered, the search is continued at the next mismatch position or the read is tagged as non-NTA. After detecting all NTA reads, we calculate the weighted mean per sample by dividing the number of reads ending with NTAs of a given nucleobase (A, U, C, and G) by total number of reads mapped to miRNAs. Per miRNA and per sample, we computed the total number of reads ending with NTAs of a given nucleobase, in addition to the total number of reads mapped to that miRNA. So, for each nucleobase, we could use the number of reads, in relation to the total, in a logistic regression model that also included the sample type (cell or exosome) as well as the cell line (accounting for the paired design). Based upon this model, we extracted p values for the difference between proportions of miRNA counts with NTA of a given nucleotide and between cells and exosomes. After fitting this model per miRNA, Benjamini-Hochberg's FDR is applied to the p values in order to correct for multiple testing.

Distribution of Small RNAs with Nontemplated Nucleotides Additions

The assessment of the distribution of posttranscriptionally modified reads (NTAs) between cells and exosomes was performed as following. To test if miRNA-related reads have a tendency either to be enriched in exosomes or to be enriched in cells, we compared those to the baseline distribution tendency of the given miRNA (defined by canonical reads). We define the enrichment coefficient by computing the ratio of the fold changes between exosomes and cells for reads ending with a certain type of nontemplated nucleotide (defined as NTA) and those without terminal modification (defined as noNTA). The coefficient will be close to 0, for which the NTA reads and the non-NTA reads of a small ncRNA sequence have the equal tendency to be associated with cells and with exosomes. It will be positive if the NTA reads have a stronger tendency to be enriched in exosomes compared to the non-NTA reads. Finally, a negative coefficient indicates that NTA reads have a stronger tendency to be enriched in cells compared to non-NTA reads.

$$EC = \log_2\left(\frac{RC_{Exo}}{RC_{cell}} \Big/ Baseline\right) \quad Baseline = \frac{RC_{exo}^{canonical}}{RC_{cell}^{canonical}}$$

ACCESSION NUMBERS

The NCBI SRA accession number for the small RNA sequencing by Illumina HiSeq 2000 reported in this paper is SRP046046.

SUPPLEMENTAL INFORMATION

Supplemental Information includes Supplemental Experimental Procedures, four figures, and two tables and can be found with this article online at http://dx.doi.org/10.1016/j.celrep.2014.08.027.

AUTHOR CONTRIBUTIONS

This study was conceived by D.K.-L., M.H., and D.M.P. D.K.-L., M.H., and D.M.P. designed experiments and analyzed and interpreted the data; M.H. did all bioinformatics analyses; and R.X.d.M. did statistical analyses. I.V.B. prepared exosomes fractions from urine for RNA-seq and carried out biological pathway analysis. D.K.-L., P.S., and M.A.J.v.E. carried out exosomes preparations from cultured B cells and performed RT-PCR experiments. D.K.-L. and D.S. supervised RNA-seq procedures. J.M.M., T.W., and B.Y. provided reagents. J.M.M., B.Y., T.W., and G.A.M. provided critical feedback. D.K.-L. and D.M.P. wrote the manuscript.

ACKNOWLEDGMENTS

We thank P.P. Eijk, F. Rustenburg, and Y. Sabogal Piñeros for their technical assistance and J. Berenguer de Felipe for inspiring discussions. T.W. is supported by VIDI 91711366. D.M.P. is supported by personal Dutch Cancer Society research award (KWF-5510). This work was funded by AICR grant 11-0157 and NWO-VENI 91696087 awarded to D.M.P.

Received: July 31, 2013
Revised: March 25, 2014
Accepted: August 13, 2014
Published: September 18, 2014

REFERENCES

Amaral, P.P., Dinger, M.E., Mercer, T.R., and Mattick, J.S. (2008). The eukaryotic genome as an RNA machine. Science *319*, 1787–1789.

Ameres, S.L., and Zamore, P.D. (2013). Diversifying microRNA sequence and function. Nat. Rev. Mol. Cell Biol. *14*, 475–488.

Ameres, S.L., Martinez, J., and Schroeder, R. (2007). Molecular basis for target RNA recognition and cleavage by human RISC. Cell *130*, 101–112.

Ameres, S.L., Horwich, M.D., Hung, J.-H., Xu, J., Ghildiyal, M., Weng, Z., and Zamore, P.D. (2010). Target RNA-directed trimming and tailing of small silencing RNAs. Science *328*, 1534–1539.

Arroyo, J.D., Chevillet, J.R., Kroh, E.M., Ruf, I.K., Pritchard, C.C., Gibson, D.F., Mitchell, P.S., Bennett, C.F., Pogosova-Agadjanyan, E.L., Stirewalt, D.L., et al. (2011). Argonaute2 complexes carry a population of circulating microRNAs independent of vesicles in human plasma. Proc. Natl. Acad. Sci. USA *108*, 5003–5008.

Baccarini, A., Chauhan, H., Gardner, T.J., Jayaprakash, A.D., Sachidanandam, R., and Brown, B.D. (2011). Kinetic analysis reveals the fate of a microRNA following target regulation in mammalian cells. Curr. Biol. *21*, 369–376.

Balaj, L., Lessard, R., Dai, L., Cho, Y.-J., Pomeroy, S.L., Breakefield, X.O., and Skog, J. (2011). Tumour microvesicles contain retrotransposon elements and amplified oncogene sequences. Nat. Commun. *2*, 180.

Bellingham, S.A., Coleman, B.M., and Hill, A.F. (2012). Small RNA deep sequencing reveals a distinct miRNA signature released in exosomes from prion-infected neuronal cells. Nucleic Acids Res. *40*, 10937–10949.

Boele, J., Persson, H., Shin, J.W., Ishizu, Y., Newie, I.S., Søkilde, R., Hawkins, S.M., Coarfa, C., Ikeda, K., Takayama, K., et al. (2014). PAPD5-mediated 3′ adenylation and subsequent degradation of miR-21 is disrupted in proliferative disease. Proc. Natl. Acad. Sci. USA *111*, 11467–11472.

Burroughs, A.M., Ando, Y., de Hoon, M.J.L., Tomaru, Y., Nishibu, T., Ukekawa, R., Funakoshi, T., Kurokawa, T., Suzuki, H., Hayashizaki, Y., and Daub, C.O. (2010). A comprehensive survey of 3′ animal miRNA modification events and a possible role for 3′ adenylation in modulating miRNA targeting effectiveness. Genome Res. *20*, 1398–1410.

Chairoungdua, A., Smith, D.L., Pochard, P., Hull, M., and Caplan, M.J. (2010). Exosome release of β-catenin: a novel mechanism that antagonizes Wnt signaling. J. Cell Biol. *190*, 1079–1091.

Chitwood, D.H., and Timmermans, M.C.P. (2010). Small RNAs are on the move. Nature *467*, 415–419.

D'Ambrogio, A., Gu, W., Udagawa, T., Mello, C.C., and Richter, J.D. (2012). Specific miRNA stabilization by Gld2-catalyzed monoadenylation. Cell Reports *2*, 1537–1545.

Fernandez-Valverde, S.L., Taft, R.J., and Mattick, J.S. (2010). Dynamic isomiR regulation in Drosophila development. RNA *16*, 1881–1888.

Garcia, E.L., Onafuwa-Nuga, A., Sim, S., King, S.R., Wolin, S.L., and Telesnitsky, A. (2009). Packaging of host mY RNAs by murine leukemia virus may occur early in Y RNA biogenesis. J. Virol. *83*, 12526–12534.

Gibbings, D.J., Ciaudo, C., Erhardt, M., and Voinnet, O. (2009). Multivesicular bodies associate with components of miRNA effector complexes and modulate miRNA activity. Nat. Cell Biol. *11*, 1143–1149.

Gibbings, D., Mostowy, S., Jay, F., Schwab, Y., Cossart, P., and Voinnet, O. (2012). Selective autophagy degrades DICER and AGO2 and regulates miRNA activity. Nat. Cell Biol. *14*, 1314–1321.

Guasparri, I., Bubman, D., and Cesarman, E. (2008). EBV LMP2A affects LMP1-mediated NF-kappaB signaling and survival of lymphoma cells by regulating TRAF2 expression. Blood *111*, 3813–3820.

Jones, M.R., Quinton, L.J., Blahna, M.T., Neilson, J.R., Fu, S., Ivanov, A.R., Wolf, D.A., and Mizgerd, J.P. (2009). Zcchc11-dependent uridylation of microRNA directs cytokine expression. Nat. Cell Biol. *11*, 1157–1163.

Katoh, T., Sakaguchi, Y., Miyauchi, K., Suzuki, T., Kashiwabara, S., Baba, T., and Suzuki, T. (2009). Selective stabilization of mammalian microRNAs by 3′ adenylation mediated by the cytoplasmic poly(A) polymerase GLD-2. Genes Dev. *23*, 433–438.

Koppers-Lalic, D., Hogenboom, M.M., Middeldorp, J.M., and Pegtel, D.M. (2013). Virus-modified exosomes for targeted RNA delivery; a new approach in nanomedicine. Adv. Drug Deliv. Rev. *65*, 348–356.

Kosaka, N., Iguchi, H., Hagiwara, K., Yoshioka, Y., Takeshita, F., and Ochiya, T. (2013). Neutral sphingomyelinase 2 (nSMase2)-dependent exosomal transfer of angiogenic microRNAs regulate cancer cell metastasis. J. Biol. Chem. *288*, 10849–10859.

Lee, Y.S., Pressman, S., Andress, A.P., Kim, K., White, J.L., Cassidy, J.J., Li, X., Lubell, K., Lim, H., Cho, I.S., et al. (2009). Silencing by small RNAs is linked to endosomal trafficking. Nat. Cell Biol. *11*, 1150–1156.

Martens-Uzunova, E.S., Olvedy, M., and Jenster, G. (2013). Beyond microRNA—novel RNAs derived from small non-coding RNA and their implication in cancer. Cancer Lett. *340*, 201–211.

Martin, G., and Keller, W. (2007). RNA-specific ribonucleotidyl transferases. RNA *13*, 1834–1849.

Mittelbrunn, M., and Sánchez-Madrid, F. (2012). Intercellular communication: diverse structures for exchange of genetic information. Nat. Rev. Mol. Cell Biol. *13*, 328–335.

Mittelbrunn, M., Gutiérrez-Vázquez, C., Villarroya-Beltri, C., González, S., Sánchez-Cabo, F., González, M.Á., Bernad, A., and Sánchez-Madrid, F. (2011). Unidirectional transfer of microRNA-loaded exosomes from T cells to antigen-presenting cells. Nat. Commun. *2*, 282.

Morin, R.D., O'Connor, M.D., Griffith, M., Kuchenbauer, F., Delaney, A., Prabhu, A.-L., Zhao, Y., McDonald, H., Zeng, T., Hirst, M., et al. (2008). Application of massively parallel sequencing to microRNA profiling and discovery in human embryonic stem cells. Genome Res. *18*, 610–621.

Mullokandov, G., Baccarini, A., Ruzo, A., Jayaprakash, A.D., Tung, N., Israelow, B., Evans, M.J., Sachidanandam, R., and Brown, B.D. (2012). High-throughput assessment of microRNA activity and function using microRNA sensor and decoy libraries. Nat. Methods *9*, 840–846.

Nolte-'t Hoen, E.N.M., Buermans, H.P.J., Waasdorp, M., Stoorvogel, W., Wauben, M.H.M., and 't Hoen, P.A.C. (2012). Deep sequencing of RNA from immune cell-derived vesicles uncovers the selective incorporation of small non-coding RNA biotypes with potential regulatory functions. Nucleic Acids Res. *40*, 9272–9285.

Okoye, I.S., Coomes, S.M., Pelly, V.S., Czieso, S., Papayannopoulos, V., Tolmachova, T., Seabra, M.C., and Wilson, M.S. (2014). MicroRNA-Containing T-Regulatory-Cell-Derived Exosomes Suppress Pathogenic T Helper 1 Cells. Immunity *41*, 89–103.

Pegtel, D.M., Cosmopoulos, K., Thorley-Lawson, D.A., van Eijndhoven, M.A.J., Hopmans, E.S., Lindenberg, J.L., de Gruijl, T.D., Würdinger, T., and Middeldorp, J.M. (2010). Functional delivery of viral miRNAs via exosomes. Proc. Natl. Acad. Sci. USA *107*, 6328–6333.

Pegtel, D.M., van de Garde, M.D.B., and Middeldorp, J.M. (2011). Viral miRNAs exploiting the endosomal-exosomal pathway for intercellular cross-talk and immune evasion. Biochim. Biophys. Acta *1809*, 715–721.

Polikepahad, S., and Corry, D.B. (2013). Profiling of T helper cell-derived small RNAs reveals unique antisense transcripts and differential association of miRNAs with argonaute proteins 1 and 2. Nucleic Acids Res. *41*, 1164–1177.

Qiu, J., Cosmopoulos, K., Pegtel, M., Hopmans, E., Murray, P., Middeldorp, J., Shapiro, M., and Thorley-Lawson, D.A. (2011). A novel persistence associated EBV miRNA expression profile is disrupted in neoplasia. PLoS Pathog. *7*, e1002193.

Riley, K.J., Rabinowitz, G.S., Yario, T.A., Luna, J.M., Darnell, R.B., and Steitz, J.A. (2012). EBV and human microRNAs co-target oncogenic and apoptotic viral and human genes during latency. EMBO J. *31*, 2207–2221.

Robinson, M.D., McCarthy, D.J., and Smyth, G.K. (2010). edgeR: a Bioconductor package for differential expression analysis of digital gene expression data. Bioinformatics *26*, 139–140.

Saito, Y., Liang, G., Egger, G., Friedman, J.M., Chuang, J.C., Coetzee, G.A., and Jones, P.A. (2006). Specific activation of microRNA-127 with downregulation of the proto-oncogene BCL6 by chromatin-modifying drugs in human cancer cells. Cancer Cell *9*, 435–443.

Scott, D.D., and Norbury, C.J. (2013). RNA decay via 3′ uridylation. Biochim. Biophys. Acta *1829*, 654–665.

Seto, E., Moosmann, A., Grömminger, S., Walz, N., Grundhoff, A., and Hammerschmidt, W. (2010). Micro RNAs of Epstein-Barr virus promote cell cycle progression and prevent apoptosis of primary human B cells. PLoS Pathog. *6*, e1001063.

Song, L., Lin, C., Gong, H., Wang, C., Liu, L., Wu, J., Tao, S., Hu, B., Cheng, S.-Y., Li, M., and Li, J. (2013). miR-486 sustains NF-κB activity by disrupting multiple NF-κB-negative feedback loops. Cell Res. *23*, 274–289.

Verweij, F.J., van Eijndhoven, M.A.J., Middeldorp, J., and Pegtel, D.M. (2013). Analysis of viral microRNA exchange via exosomes in vitro and in vivo. Methods Mol. Biol. *1024*, 53–68.

Villarroya-Beltri, C., Gutiérrez-Vázquez, C., Sánchez-Cabo, F., Pérez-Hernández, D., Vázquez, J., Martin-Cofreces, N., Martinez-Herrera, D.J., Pascual-Montano, A., Mittelbrunn, M., and Sánchez-Madrid, F. (2013). Sumoylated hnRNPA2B1 controls the sorting of miRNAs into exosomes through binding to specific motifs. Nat. Commun. *4*, 2980.

Vojtech, L., Woo, S., Hughes, S., Levy, C., Ballweber, L., Sauteraud, R.P., Strobl, J., Westerberg, K., Gottardo, R., Tewari, M., and Hladik, F. (2014). Exosomes in human semen carry a distinctive repertoire of small non-coding RNAs with potential regulatory functions. Nucleic Acids Res. *42*, 7290–7304.

Wee, L.M., Flores-Jasso, C.F., Salomon, W.E., and Zamore, P.D. (2012). Argonaute divides its RNA guide into domains with distinct functions and RNA-binding properties. Cell *151*, 1055–1067.

Wyman, S.K., Knouf, E.C., Parkin, R.K., Fritz, B.R., Lin, D.W., Dennis, L.M., Krouse, M.A., Webster, P.J., and Tewari, M. (2011). Post-transcriptional generation of miRNA variants by multiple nucleotidyl transferases contributes to miRNA transcriptome complexity. Genome Res. *21*, 1450–1461.

Yao, B., La, L.B., Chen, Y.-C., Chang, L.-J., and Chan, E.K.L. (2012). Defining a new role of GW182 in maintaining miRNA stability. EMBO Rep. *13*, 1102–1108.